Acoustic Light Modulators Using Optical Heterodyne Mixing

By R. W. DIXON and E. I. GORDON

(Manuscript received September 21, 1966)

Acoustic light modulators are discussed in which the optical carrier is reinserted in the diffracted, frequency-shifted light beam. Reinsertion is accomplished in a novel fashion using a Kösters prism. In contrast to the usual acoustic modulator, the diffracted light is power modulated at the acoustic frequency. Modulation bandwidth and depth are each calculated as a function of the optical and acoustic beam parameters, assuming a Gaussian optical beam and rectangular acoustic beam. It is shown that the modulation bandwidth increases proportional to the optical beam diffraction angle and equals the inverse of the transit time of the sound across the waist of the optical beam. The optimum modulation depth, for a given acoustic power, corresponds to approximate equality of the optical and acoustic diffraction angles. Confirming experiments in the frequency range 250/350 MHz are described.

I. INTRODUCTION

Detection of optical radiation using heterodyne mixing was pioneered in the classic experiments of Forrester, Gudmundsen, and Johnson.[1] They successfully detected the microwave beat between two Zeeman components of a mercury arc. With coherent light sources the technique was utilized initially in the investigation of the mode structure and frequency stability of the helium-neon laser.[2] Subsequently, optical heterodyne mixing has been used as a sensitive, high-resolution detector of frequency shifts in the study of Brillouin scattering[3] and of the frequency broadening of Rayleigh scattered light.[4]

It is well known that under the correct circumstances an optical beam, passing through a transparent material containing a traveling acoustic wave, has part of its energy diffracted by the refractive index variations associated with the acoustic wave. In the proper range of parameters, known as the Bragg region, the diffracted light is con-

fined around a single direction. The system acts as a single-sideband suppressed-carrier modulator in which the diffracted light is intensity modulated with the envelope of the modulation subcarrier. Depending on the relative directions of the light and sound the diffracted light frequency is increased or decreased by the frequency of the modulation subcarrier.

One may arrange to have the diffracted light fall into the same solid angle as a portion of the original light, and thereby allow detection of the diffracted beam by heterodyne mixing with the undiffracted beam. Heterodyne mixing of light in which the signal frequency is shifted by diffraction from sound in a liquid cell ultrasonic modulator has been demonstrated by Cummins and Knable,[5] and the increased sensitivity of this technique has been briefly pointed out by Goodwin and Pedinoff.[6]

Optical heterodyne procedures in combination with Bragg scattering can also be used as a sensitive detector of sound. For example, Lastovska and Benedek[3] have shown that thermal sound (thermal Brillouin scattering) may be detected in this way. In fact, in some applications—e.g., at very high frequencies—this technique can be a more sensitive detector of sound than the best available transducer. The advantages of optical techniques for investigating sound beam intensity profiles, angular distributions, etc. at any point in the medium in which the acoustic wave propagates have been pointed out earlier[7] and may now be supplemented by the increased sensitivity and spectral range which the utilization of optical heterodyne detection affords. An additional advantage of this method of optical detection is that solid-state photodetectors may be used instead of photomultipliers, without compromising sensitivity, whenever sufficient light is available that the shot noise associated with the optical local oscillator limits detector sensitivity.[8]

This paper is concerned with the detailed properties of an acoustic modulator when optical heterodyne detection of the modulated light is employed. A coherent optical source is assumed. The range of useful modulation frequencies for this technique extends at present well into the microwave region. Present limitations of efficient thin-film transducers limit operation to below 10 GHz. Acoustic loss for some applications becomes important at lower frequencies than this. The frequency response of commercial photodiodes extends to about 30 GHz.

The analysis includes a discussion of modulation bandwidth and optimum modulation conditions and concludes with the prediction that

very large dynamic bandwidths may be obtained using optical heterodyne mixing in conjunction with an acoustic modulator. A series of experiments involving a novel beam splitter and various modulating materials confirm this prediction. It is shown that bandwidth is related to the diffraction angle of the optical beam and may be varied over a large range by changing this angle. Experiments have been restricted to solid modulating materials, but the results are applicable without modification to liquids if their higher acoustic loss can be accepted. It is concluded that large modulation depths should be practical at modulation frequencies well into the microwave region and at optical frequencies throughout the visible and infrared. It is also pointed out that for small diffracted light intensities, proportionately much larger modulation depths are possible using this technique than if the transmitted light beam alone were monitored.

The relation of modulation depth and bandwidth for a given acoustic power is discussed, and experimental confirmation of the conclusions is presented. In addition, it is shown that with these acoustic light modulators frequency and phase information, as well as power modulation, may be transferred to the light with large dynamic bandwidth.

II. DISCUSSION

2.1 *Optical Beam Geometry*

In order to obtain two beams for use in optical heterodyne mixing experiments, it has been common practice to use a beam splitter and mirror assembly similar to that shown schematically in Fig. 1. The configuration shown would be appropriate for coherent detection of light modulated by Bragg diffraction from an acoustic wave.[5] In the experiments described here it has been found very useful to replace the mirror and beam splitter of such an experiment with a Kösters prism.[9] These prisms have been commonly used in Michelson interferometers and similar apparatus where ease of alignment is desired.[10] Probably this prism has not received the attention it deserves for applications in modern physical experiments.

Fig. 2 shows the general construction of a Kösters prism. Two accurately constructed 30-60-90° prisms are carefully cemented together with a dielectric beam splitter between them. Because the two exit beams travel symmetrical paths to their intersection with any plane perpendicular to the beam splitter, they are optically identical.

The experimental apparatus used in the present series of experiments is shown schematically in Fig. 3. The two beams from the Kösters

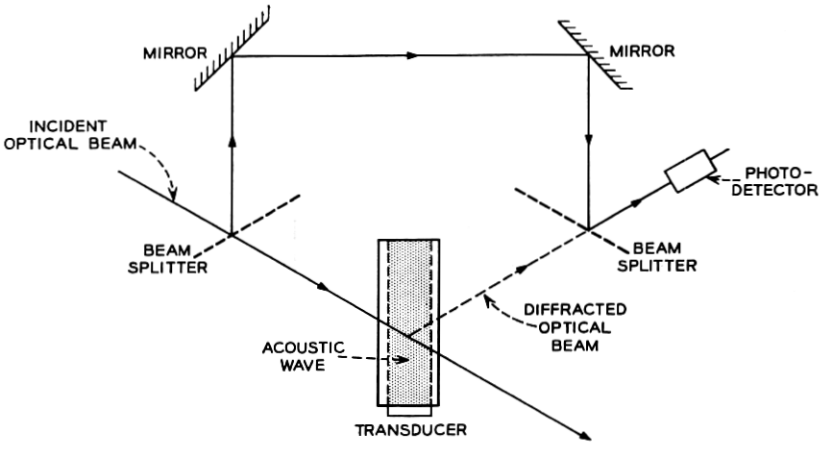

Fig. 1 — Mirrors and beam splitters arranged for optical heterodyne detection of Bragg diffracted light (after Cummins and Knable, Ref. 5).

prism are set to intersect within the acoustic beam at an angle equal to twice the Bragg angle so that Bragg diffracted light from each of the incident beams falls into the diffraction angle of the other beam. The Kösters prism assures symmetrical paths for the diffracted and undiffracted light and thereby makes alignment very easy. A lens of appropriate focal length is positioned so that the optical beam waists intersect with the desired convergence angle in the center of the modulator's acoustic beam.

Consider, in Fig. 3, an acoustic traveling wave originating from the transducer. The frequency of the light diffracted from beam 1 into beam 2 is increased by the acoustic frequency while the light diffracted

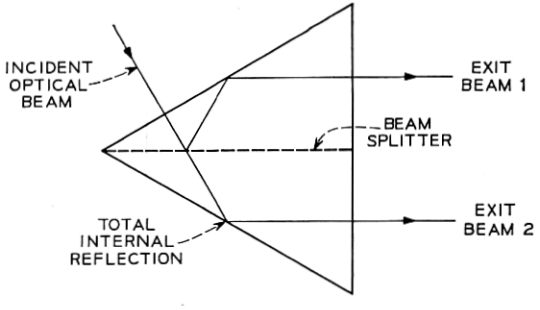

Fig. 2 — A Kösters prism or double image beam splitter.

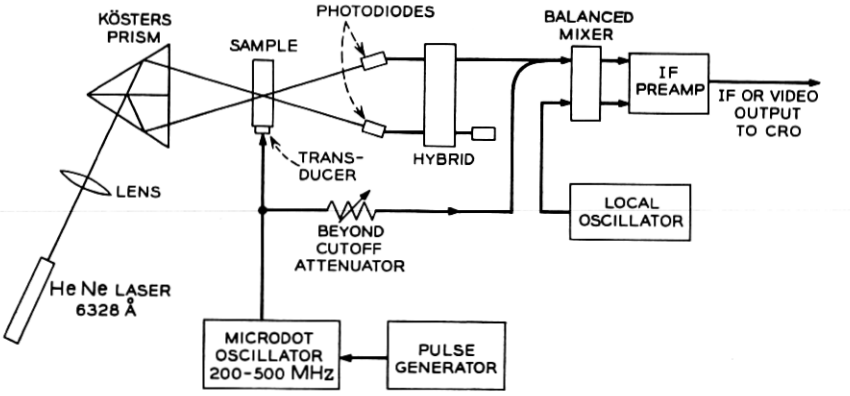

Fig. 3 — Schematic diagram of experimental apparatus.

from beam 2 into beam 1 is decreased by the same amount. The diffracted and transmitted beams interfere at the photodiodes after which the difference frequencies are amplified and detected. Since the difference frequency signal from diode 1 is 180 degrees out of phase with that from diode 2, the two signals may be fed, if desired, into a hybrid and will add at the port for which the output is the difference between the two inputs (the push-pull output). This has the advantage, which was not important in the present experiments but which might be for some applications, that amplitude noise on the incident optical beam (such as the beating of various laser modes) does not appear at the same output as the detected signal if the two sides of the detection system are balanced. In some of the experiments discussed only one diode was used, in others the balanced system worked very well and was no more difficult to align than the system employing a single diode. Modulation frequencies were normally near 300 MHz.

2.2 *Modulator Bandwidth*

In order to appreciate the limits on modulation bandwidth, it is instructive to consider qualitatively several special cases. For simplicity, assume that only photodiode 2 is used and that only an outgoing acoustic wave is present. The Kösters prism is positioned so that the two light beams of frequency ν which are incident on the acoustic modulator have their point of intersection at the center of the acoustic beam. They intersect at twice the Bragg angle, $2\theta_o$, [$\sin \theta_o = \frac{1}{2} f_o \lambda / v$], which is a function of the desired modulator center frequency f_o, the acoustic velocity v, and the optical wavelength in the medium λ. The optical

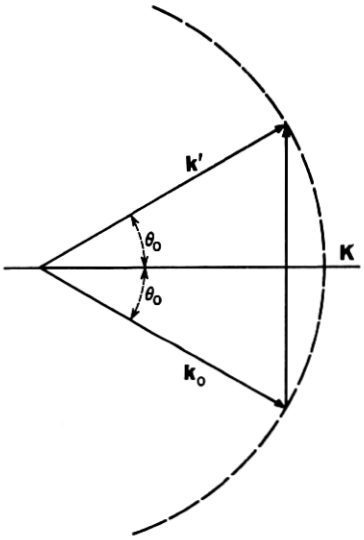

Fig. 4 — A k-vector diagram of the Bragg diffraction process in which optical and acoustic diffraction angles are assumed negligibly small.

velocity is c'. The wave vector relation (momentum conservation) among the three waves may be written $\mathbf{k}_o + \mathbf{K} = \mathbf{k}'$, where $|\mathbf{k}_o| = 2\pi\nu/c'$ and $|\mathbf{k}'| = 2\pi(\nu + f_o)/c'$ are the incident and scattered optical k-vectors, and $\mathbf{K}$ is the k-vector of the ultrasonic wave. Since to order $|f_o/\nu| \ll 1$, $|\mathbf{k}_o| = |\mathbf{k}'|$ it is possible to make the elementary but useful construction shown in Fig. 4. The dotted circle has radius $|\mathbf{k}_o|$ and defines the locus of allowed $|\mathbf{k}'|$. Only a phonon of precisely the correct $|\mathbf{K}|$ will scatter $\mathbf{k}_o$ if one assumes that neither the optical nor acoustic beam has any angular width.

In order to appreciate the effect of nonzero diffraction angle, consider the limiting case in which the diffraction angle of the acoustic beam is large compared with the diffraction angle of the optical beam (Fig. 5); $\mathbf{K}$ has a well-defined magnitude but an angular width $\Delta\theta$. Only those acoustic k-vectors near the direction of $\mathbf{K}_o$ scatter light into spatial coherence with the heterodyning beam $\mathbf{k}_o'$. Thus, the detected signal amplitude is lower than if the same acoustic power were confined to a smaller diffraction angle.

If the acoustic frequency is increased to a new value, $|\mathbf{K}|$ is increased and the construction shown dashed is appropriate. No signal will be observed on the photodiode because no $\mathbf{K}$ can scatter into $\mathbf{k}_o'$. This

modulator therefore, not only produces low modulation intensity but also possesses small bandwidth.

Now consider the other limiting case in which the diffraction angle of the optical beam is much larger than that of the acoustic beam (Fig. 6). In this case, only that portion of the optical energy near the center of the diffraction angle can be scattered by the acoustic wave of vector $\mathbf{K}_o$ and heterodyned with the other optical wave. Therefore, the scattered intensity is much less than it would be for the same optical and acoustic powers, if the diffraction angle of the light were decreased.

If the frequency f_o is changed slightly, a new $\mathbf{K}$ is defined which is slightly different in magnitude but which has the same direction as $\mathbf{K}_o$. In this case, however, the detected optical signal at the photodiode is essentially unchanged as long as the deviation ΔK is such that $K_o + \Delta K$ still connects two points on the dashed circle which are within the diffraction angles of the incident and hetrodyning optical beams. By varying f one traces out the angular profile of the *optical* beam. A bandwidth may be approximately defined by the condition

$$\{ \mid K_{\max} \mid - \mid K_{\min} \mid \} \approx \sqrt{2}\, \Delta\theta_o k_o \cos\theta_o \tag{1}$$

from which it follows that the bandwidth Δf_B is given by

$$\Delta f_B \approx \sqrt{2}\, (v/\lambda)\, \Delta\theta_o \cos\theta_o \tag{2}$$

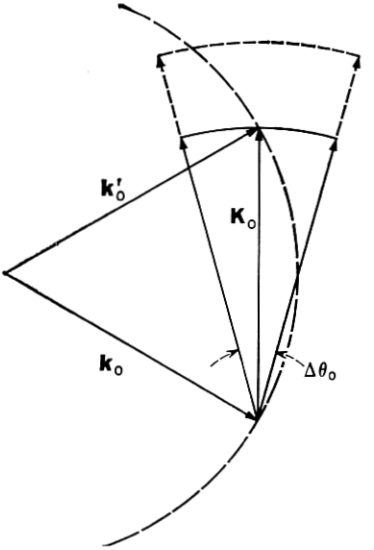

Fig. 5 — A k-vector diagram of the Bragg diffraction process in which the acoustic diffraction angle is large compared with the optical diffraction angle.

in which λ is the optical wavelength. The center frequency f_o is defined by $\sin \theta_o = \frac{1}{2} f_o v/\lambda$. The optical beam diffraction angle $\Delta\theta_o$ may be expressed in terms of the beam waist diameter w_o,[11] corresponding to a Gaussian beam for which w_o is the full width at half intensity,

$$w_o \, \Delta\theta_o \approx \lambda\left(\frac{2 \ln 2}{\pi}\right). \tag{3}$$

Substituting for $\Delta\theta_o$ yields for the bandwidth

$$\Delta f_B \approx \left(\frac{2\sqrt{2} \ln 2}{\pi}\right) \frac{v \cos \theta_o}{w_o} \tag{4}$$

which approximates the reciprocal of the transit time of the sound across the waist of the gaussian light beam. This important result shows how acoustic modulators with large bandwidths are made possible by increasing the diffraction angle of the optical beam. The fact that the diffraction angle $\Delta\theta_o$ of the optical beam must be less than the Bragg angle requires that the fractional bandwidth of the modulator obeys the inequality, using (2) and (3),

$$\frac{\Delta f_B}{f_o} < \frac{1}{\sqrt{2}}. \tag{5}$$

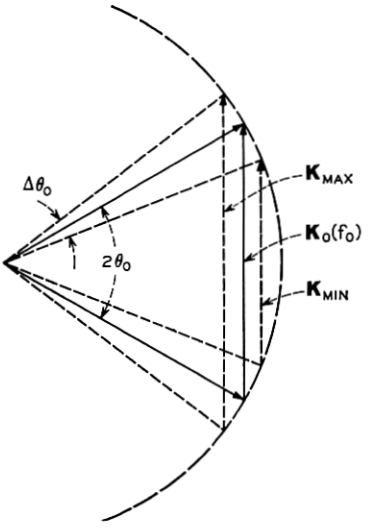

Fig. 6 — A k-vector diagram of the Bragg diffraction process showing the origin of acoustic modulator bandwidth; the optical diffraction angle is large compared with the acoustic diffraction angle.

Thus, fractional bandwidths as large as 70 percent are possible if transducer bandwidths can be made compatable with this requirement.

It should be clear now for the situation depicted in Fig. 6 that increasing the acoustic diffraction angle would increase the detected signal without affecting the bandwidth. Likewise, from Fig. 5, in the other extreme the beat signal increases but the bandwidth is unchanged when the acoustic diffraction angle is decreased. It is therefore, plausible on the basis of the foregoing comments that the choice of *acoustic diffraction angle approximately equal to optical diffraction angle* is the optimum choice for a given bandwidth. The bandwidth is determined entirely by the diffraction angle of the optical beam. This conclusion is given quantitative expression in Appendix A.

III. THEORY AND COMPARISON WITH EXPERIMENT

In order to check the preceding ideas quantitatively, the photodiode current which would be expected with the geometry shown in Fig. 3 was calculated for the case of light beams with identical Gaussian profiles and an acoustic beam with rectangular cross section. It was known that these beam profiles could be accurately approximated experimentally. The lens was positioned in the incident optical beam so that the optical beam waist occurred at the center of the modulator. The diode photocurrent was computed as the far-field interference integral of the product of the acoustically diffracted optical amplitude and the heterodyning optical amplitude. Details of the calculation are presented in Appendix A. The expression for the component of photocurrent at the modulating frequency f, apart from material and numerical constants, is

$$\iota(f) = -\frac{i}{(\sin\theta_o)^{\frac{1}{2}}} P_{\text{opt}}(P_{\text{acoustic}})^{\frac{1}{2}} \exp\left[i2\pi f(t - R/c')\right] \cdot \frac{\text{Erf}\,(a)}{a^{\frac{1}{2}}} \cdot \frac{\text{Erf}\,(b)}{b^{\frac{1}{2}}} \cdot \exp\left[-\frac{\pi^2}{4\ln 2}\frac{(f - f_o)^2 w_o^2}{v^2\cos^2\theta_o}\right], \quad (6)$$

where

$$a \equiv \left(\frac{\ln 2}{2}\right)^{\frac{1}{2}} \frac{h}{w_o}$$

$$b \equiv (\ln 2)^{\frac{1}{2}} \frac{L\sin\theta_o}{w_o}$$

$$\sin\theta_o \equiv \frac{1}{2}\frac{f_o\lambda}{v}.$$

Again w_o is the full width at half intensity of the Gaussian beam, $2\theta_o$ is the intersection angle inside the modulating medium and f_o is the acoustic frequency for which θ_o is the Bragg angle. The acoustic beam height is h and its width (dimension in the plane formed by the acoustic and optic propagation directions) is L. The distance to the detector is R. Equation (6) is the basic relation which is subject to experimental verification.

The first experimental checks of (6) confirmed that the acoustic and optical power dependences are correct. Experimentally, a 3-dB decrease in optical intensity or a 6-dB decrease in acoustic power as expected decreased the detected current by one-half. The other most interesting predictions made by (6) are contained in the terms $\mathrm{Erf}(b)/b^{\frac{1}{2}}$ and

$$\exp\left[-\frac{\pi^2}{4\ln 2}\frac{(f-f_o)^2 w_o^2}{v^2\cos^2\theta_o}\right].$$

The former is concerned with the maximum detected signal amplitude and the latter with the dynamic modulation bandwidth, both as functions of the diffraction angle of the incident light.

3.1 *Bandwidth vs Beam Waist Diameter*

Consider first the term

$$\exp\left[-\frac{\pi^2}{4\ln 2}\frac{(f-f_o)^2 w_o^2}{v^2\cos^2\theta_o}\right].$$

When the modulating frequency f changes from the value f_o, this term describes the decrease in detected signal. An acoustic half-power bandwidth, Δf_B, for which the detected current is greater than $1/\sqrt{2}$ below its maximum value, may be defined and is given by

$$w_o\,\Delta f_B = \left(\frac{2\sqrt{2}\ln 2}{\pi}\right) v\cos\theta_o\,. \tag{7}$$

The beam waist diameter times the bandwidth is thus a constant for a given material at a given center frequency $f_o(\theta_o)$. By making the beam waist smaller, e.g., by focusing the incident optical beam, the dynamic bandwidth may be increased. As indicated earlier the bandwidth is intimately related to the transit time of the acoustic wave across the optical beam. In fused quartz for longitudinal waves at frequencies low enough that $\cos\theta_o \approx 1$, (7) becomes

$$w_o\,\Delta f_B = 3.70 \times 10^5 \text{ cm/sec}. \tag{8}$$

In Fig. 7 the measured bandwidth Δf_B, for modulation in fused quartz, is plotted against w_o^{-1} and (8) is shown plotted as the solid line. The

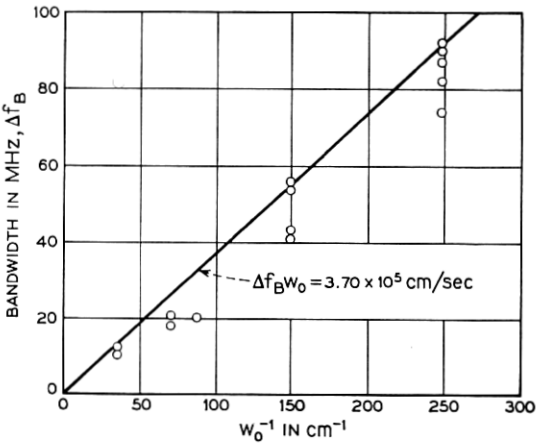

Fig. 7 — Experimental dynamic bandwidth plotted against the reciprocal of the optical beam waist diameter. The solid line is the theoretical expression, (8).

value of w_o was varied by placing lenses of different focal lengths F in the incident optical beam. The relation between w_o and F was assumed to be of the form given by Kogelnik[11] except that w_o is defined as the full width at half intensity of the Gaussian beam. In the limit appropriate for the present experiments

$$w_o \approx \left(\frac{2 \ln 2}{\pi}\right) \frac{F\lambda_o}{W_o}, \tag{9}$$

in which W_o is the beam waist of the incident laser beam and w_o is the beam waist of the beam in the scattering medium following its transformation by a lens of focal length F. Here, λ_o is the free space wavelength. Equation (9) was used to convert from values of F to values of w_o. Using a scanning slit and photomultiplier the value $W_o = (1.00 \pm 0.01)$mm was found. These measurements incidentally verified that the intensity profile of the laser beam was approximately Gaussian.

The experimental points in Fig. 7 were obtained using apparatus which is shown schematically in Fig. 3. The Microdot oscillator produced repetitive pulses of RF energy with each pulse having about 1-μsec duration. Cadmium sulfide thin-film transducers converted these electromagnetic pulses into acoustic energy.[12] The deflected light pulses were detected in the indicated photodiode geometry followed by a standard microwave superheterodyne receiver. In order to avoid IF detector diode nonlinearity the IF output of the system was usually viewed directly on a broadband oscilloscope. Data were taken from the amplitude

of the first deflected light pulse (due to the initial outgoing acoustic wave) and were therefore, independent of acoustic resonance effects which would be associated with long acoustic pulses. The RF power incident on the transducer was kept the same at each frequency. A small amount of each RF pulse was fed, using a beyond cutoff attenuator, from in front of the transducer to the input of the receiver. This pulse served as a calibrating signal for the receiver and helped to correct for changes in receiver sensitivity as the frequency was changed. The transducer response in the 100-MHz region around 300 MHz was flat to within 1 dB. The scatter of the experimental points can be attributed to several causes, the most important of which is the unavoidable small changes in optical alignment between the time that each bandwidth curve was taken. It is believed that the largest observed value for any given value of w_o is the most appropriate and the agreement is considered to be good.

3.2 *Signal Amplitude vs Beam Waist Diameter*

Now consider the amplitude terms in (6) which involve the error functions. When $f = f_o$

$$\iota(f_o) \propto \frac{\text{Erf } (a)}{a^{\frac{1}{2}}} \quad \frac{\text{Erf } (b)}{b^{\frac{1}{2}}}, \tag{10}$$

where

$$a \equiv \left(\frac{\ln 2}{2}\right)^{\frac{1}{2}} \frac{h}{w_o}$$

$$b \equiv (\ln 2)^{\frac{1}{2}} \frac{L \sin \theta_o}{w_o}.$$

In the experiments, the acoustic beam height h was made sufficiently large (3 mm) compared with the largest beam waist ($\approx$1 mm) that $\text{Erf}(a) \approx 1$ for all values of w_o of interest. Thus, the signal current as a function of w_o is given by

$$A(w_o) = A_o w_o \text{ Erf} \left[(\ln 2)^{\frac{1}{2}} \frac{L \sin \theta_o}{w_o} \right]. \tag{11}$$

This equation is plotted as the solid curve in Fig. 8; A_o has been considered an adjustable normalizing parameter but the argument of the error function is determined using the experimental acoustic beam width of $L = 7.00$ mm. The experimental points were taken using the configuration shown in Fig. 3 and the beam waist diameter was obtained using (9). Again the agreement is quite good.

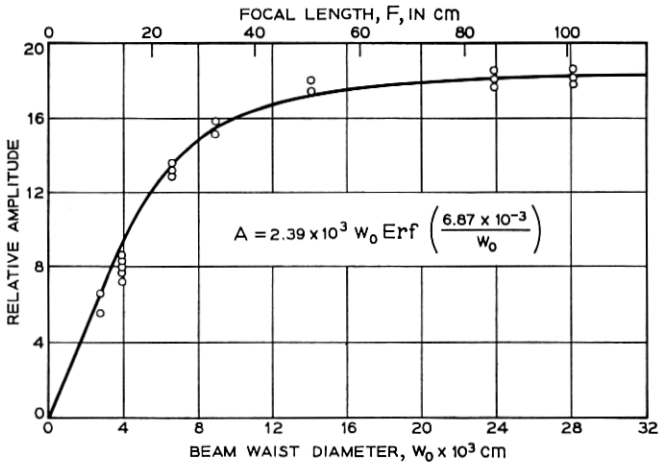

Fig. 8 — Experimental relative modulation frequency photocurrent vs beam waist diameter. The solid curve is the normalized theoretical expression, (11).

3.3 *Signal Amplitude vs Transducer Width*

The main interest thus far has been in determining the result on the signal amplitude of varying the optical diffraction angle and demonstrating that it is solely responsible for the bandwidth. It is instructive to re-emphasize the effect of the acoustic diffraction angle by calculating the detected signal variation as a function of acoustic beam width L. For a given w_o, h, θ_o and acoustic power the detected signal amplitude at $f = f_o$ is given by

$$A(L) = A_o \frac{\text{Erf}\,(b)}{b^{\frac{1}{2}}}$$
$$b = (\ln 2)^{\frac{1}{2}} \frac{L \sin \theta_o}{w_o}. \tag{12}$$

It should be noted that b can also be written as $0.85 \times$ (diffraction angle of light/diffraction angle of the sound).

In the region of small L, ($b \ll 1$)

$$A(L) = A_o(2/\pi^{\frac{1}{2}})b^{\frac{1}{2}} \propto L^{\frac{1}{2}}. \tag{13}$$

Therefore, for a given acoustic power, the signal may be increased by increasing the transducer width. The diffraction angle of the sound is too large for optimum scattering from the given optical beam. In the opposite limit of large L, ($b \gg 1$)

$$A(L) = A_o/b^{\frac{1}{2}} \propto L^{-\frac{1}{2}}. \tag{14}$$

Increasing L decreases the signal. Here, the acoustic diffraction angle is too small to use all of the incident light.

The signal amplitude has a broad maximum at $b = 0.99$ corresponding to approximate equality of the acoustic and optical diffraction angles for optimum modulator efficiency. This conclusion is expected to depend only weakly on the actual beam geometries.

IV. MODULATION DEPTH

Consider now the modulation depth which one would expect from an acoustic modulator. A simple computation of modulation depth is possible only when the waves are considered in a plane wave approximation in the Bragg region. This situation should approximate qualitatively the behavior expected with the present experimental configuration. In the Bragg region, there exists a well-defined angular relationship among the beam directions. Furthermore, all of the light diffracted from the main beam is diffracted into a single Bragg order. Under these circumstances, the solution of the problem of the generation of an optical beam by parametric coupling with an acoustic beam shows that the amplitude of the diffracted beam can be written[13]

$$P_d^{\frac{1}{2}} = \mp iP_{\text{opt}}^{\frac{1}{2}} \sin \eta^{\frac{1}{2}} \exp i2\pi(\nu \pm f)t, \tag{15}$$

while the transmitted beam has the form

$$P_t^{\frac{1}{2}} = P_{\text{opt}}^{\frac{1}{2}} \cos \eta^{\frac{1}{2}} \exp i2\pi\nu t \tag{16}$$

in which η is a scattering parameter defined for a rectangular acoustic beam by[13]

$$\eta \equiv \tfrac{1}{2}\pi^2\left(\frac{n^6p^2}{\rho v^3}\right)\left(\frac{LP_a}{\lambda_o^2 h \cos^2 \theta_o}\right), \tag{17}$$

where L is the beam width, P_a the acoustic power, h the acoustic beam height, p the appropriate photoelastic component, v the acoustic velocity, and ρ the mass density, and n the refractive index.

For conventional acoustic modulation, a square law photodetector placed in the transmitted beam will produce a photocurrent proportional to $|P_t|$ which has a maximum value of P_{opt} for no acoustic signal and a minimum value $P_{\text{opt}} \cos^2 \eta^{\frac{1}{2}}$ when the acoustic signal is present. Hence, a modulation depth

$$m_1 = \sin^2 \eta^{\frac{1}{2}} \tag{18}$$

may be defined which is some measure of the ability to detect the influence of the acoustic energy on the light.

Similarly for the superheterodyne case, the photo-current has the form

$$| P_i^{\frac{1}{2}} + P_d^{\frac{1}{2}} |^2 = P_{opt}(1 \pm \sin 2\eta^{\frac{1}{2}} \sin 2\pi ft)$$

and

$$m_2 = \frac{2 \sin 2\eta^{\frac{1}{2}}}{1 + \sin 2\eta^{\frac{1}{2}}}. \tag{19}$$

Clearly, this modulation depth is superior to that obtained when the carrier is simply intensity modulated. This superiority is most dramatic when small deflected intensities are involved. Fig. 9 shows a comparison of the two modulation depths each plotted as a function of the scattering parameter η (which for $\eta \lesssim 0.1$ is quite accurately equal to the deflected intensity). It is seen that when 10 percent deflected intensity is obtained, the modulation depth with the optical heterodyne system is 75 percent. For the very small deflected intensity of 0.01 percent, one still has a usable modulation depth of 4 percent in the optical heterodyne detector.

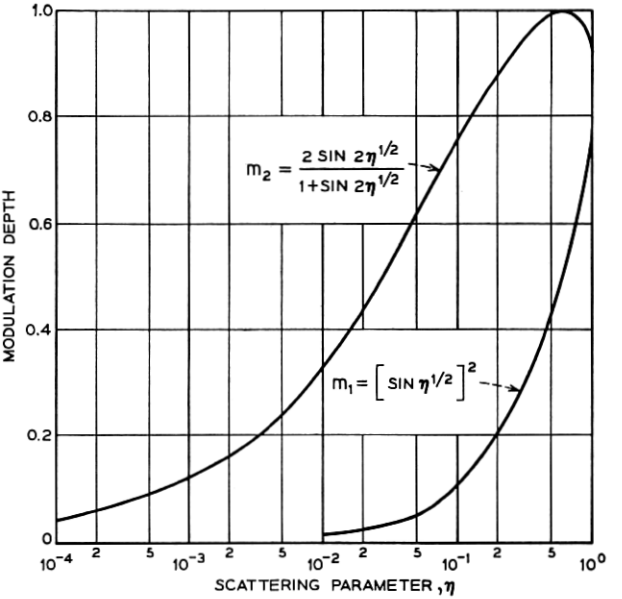

Fig. 9 — Theoretical curves, valid for plane waves, of the ordinary optical modulation depth m_1 and the optical heterodyne modulation depth m_2 both plotted vs acoustic scattering parameter η.

Modulation depth was experimentally investigated using a modulation frequency of 20 MHz which was chosen instead of a frequency near 300 MHz as in the other experiments described in this paper in order to display the modulation depth directly. At 20 MHz one photodiode could be directly connected to an oscilloscope with amplifiers having sufficient baseband bandwidth and gain to display both the dc diode photocurrent and the 20-MHz modulating photocurrent. Fig. 10 shows a typical oscilloscope trace of the diode output for longitudinal acoustic waves propagating in KRS-5 when the relative diffracted light intensity was about 20 percent. The baseline corresponds to no light. Fig. 11 shows a comparison of the modulation depth measured from such photographs compared with the total intensity diffracted from the incident beam under the same experimental conditions. KRS-5 was again the modulating medium. The very large modulation depths obtained for small diffracted intensities are, of course, the most interesting feature of these curves and qualitatively verify the ideas just discussed.

There is some disadvantage in working at a frequency as low as 20 MHz, viz., that the optical-acoustic interaction is not strictly in the Bragg region and a significant amount of light from the main optical beam is diffracted into orders other than that satisfying the Bragg condition. For this reason, the curve of m_2 against acoustic power does not reach 100 percent as it would if the modulating frequency were high enough (greater than about 60 MHz) that Bragg diffraction was dominant. At these increased frequencies a direct display of the modula-

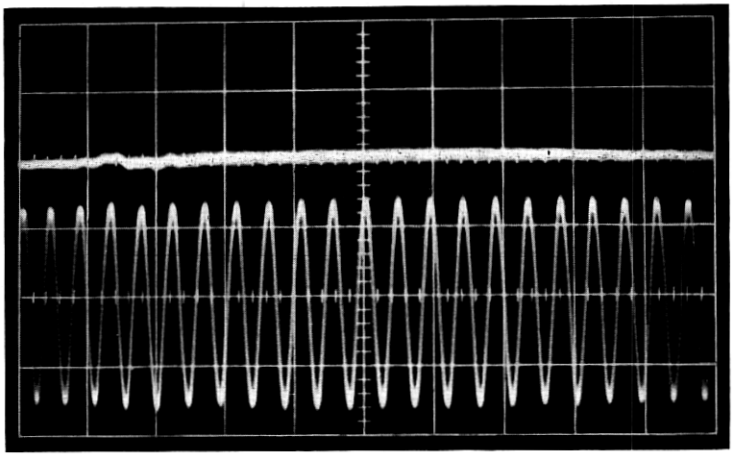

Fig. 10 — Oscilloscope trace showing 80 percent modulation depth at 20 MHz obtained using optical heterodyne detection. The relative diffracted intensity was about 20 percent.

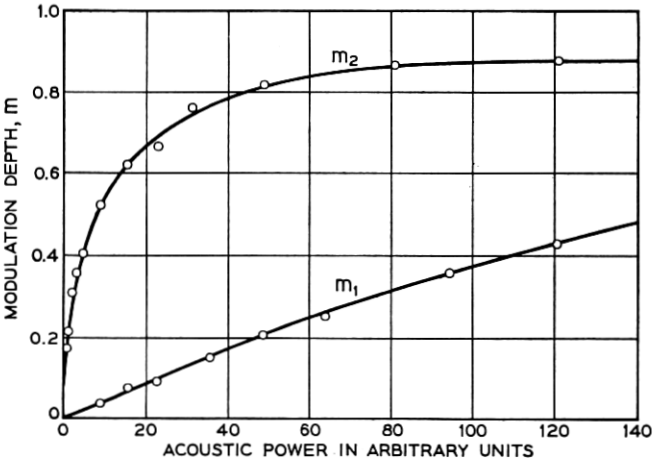

Fig. 11 — Experimental comparison of ordinary modulation depth m_1 and heterodyne modulation depth m_2 for logitudinal acoustic waves in KRS-5.

tion depth, such as that shown in Fig. 10, becomes difficult for the small photocurrents used experimentally.

V. MEASUREMENT OF ACOUSTIC DIFFRACTION PATTERN

It is known that Bragg diffraction can be used to determine the angular distribution or diffraction pattern of the acoustic beam.[7] Using a light beam sufficiently collimated that the diffraction angle of the light is much less than that of the sound, measurement of the scattered light power as a function of the angle of incidence of the light relative to the Bragg angle yields directly the angular distribution of acoustic energy. The angle of incidence is changed by slowly rocking the acoustic medium.

A similar experiment can be performed using the arrangement of Fig. 3. In this case, the component of photo-current at the acoustic frequency measures the *amplitude* of the acoustic angular distribution.

Typical results are shown in Fig. 12. Photograph (a) illustrates the case of a well-collimated light beam with diffraction angle much smaller than that of the acoustic beam, (b) and (c) are for progressively larger optical diffraction angles. In (c) the optical diffraction angle is large enough that the curve illustrates the Gaussian character of the light beam. The deviations from the expected sin X/X behavior relate to the lack of antireflection coatings on the acoustic medium.[7]

Homodyne detection of the photocurrent using the acoustic input

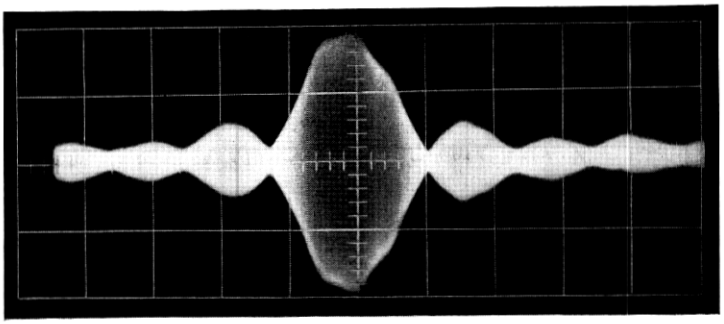

(a)

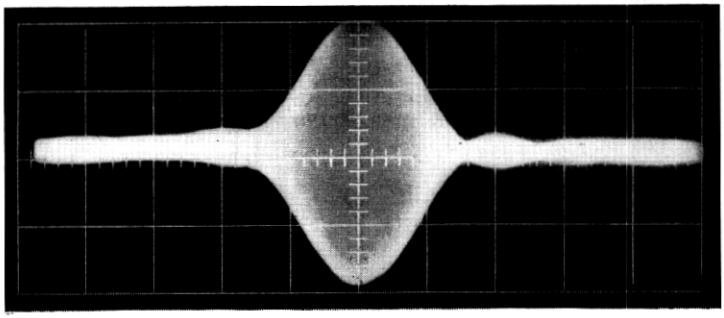

(b)

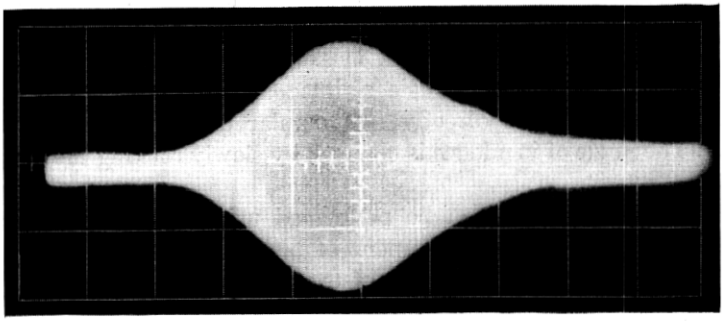

(c)

Fig. 12 — Oscilloscope display of the modulation frequency photocurrent vs angle of rotation of the modulating medium (cf., Fig. 3). Traces (a), (b), and (c) show results for increasing values of the optical beam diffraction angle.

signal as a reference would allow determination of the phase of the acoustic angular distribution as well as the amplitude. Thus, this technique has some significant advantages over the original experiments described in Ref. 7. The increased sensitivity of this technique should also be noted.

VI. CONCLUSION

A novel type of acoustic modulator arrangement has been described which allows superheterodyne detection of the diffracted light.

Distinct from electro-optic modulators, the optical modulation sidebands of acoustic devices are well separated in angle from the optical carrier and intensity modulation at the subcarrier modulation frequency is not possible. It has been shown that the optical carrier may be reinserted in the appropriate direction in a simple and convenient fashion allowing intensity modulation at the modulation frequency.

Optimum modulator configurations, corresponding to approximate equality of the optical and acoustic diffraction angles have been derived and the modulation bandwidth has been shown to be proportional to this angle or alternately to be equal to the inverse of the acoustic transit time across the optical beam waist. Confirming experiments in the frequency range 250–350 MHz have been described.

VII. ACKNOWLEDGMENT

The authors are indebted to J. S. Wagner for supplying the thin-film transducers and to D. R. Herriott and M. G. Cohen for informative conversations.

APPENDIX A

Calculation of Photodetector Output

The photodetector is usually placed in the focal plane of a collecting lens. For the purpose of calculation, one may assume that the surface of the photodetector is hemispherical, centered on the interaction volume, and sufficiently large that detection occurs in the optical far-field. The photocurrent is proportional to the instantaneous integrated intensity or power falling on the surface. The component of the power or photo-current at the acoustic frequency is proportional to the interference integral of the transmitted and diffracted optical beams.

The calculation is performed by determining the angular dependence of the transmitted and diffracted beams and integrating the product

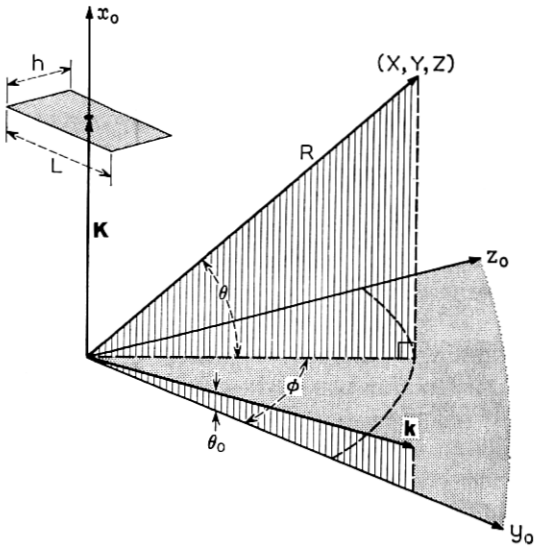

Fig. 13 — Coordinate system used in the calculation of the heterodyne photocurrent.

of the two functions on the surface of a sphere of radius R. The observation point (X, Y, Z) in Fig. 13 has coordinates

$$X = R \sin \theta$$

$$Y = R \cos \theta \cos \varphi$$

$$Z = R \cos \theta \sin \varphi.$$

The near-field amplitude distribution of the transmitted Gaussian beam which is incident in the $x_o - y_o$ plane at angle θ_o is given by

$$\psi(x_o, y_o, z_o, \theta_o)$$

$$= \psi_o \exp -\left[\frac{2 \ln 2}{w_o^2}[(x_o \cos \theta_o - y_o \sin \theta_o)^2 + z_o^2] + ik(y_o \cos \theta_o + x_o \sin \theta_o)\right], \tag{20}$$

in which w_o is the half-power beam diameter and k is the propagation constant. The amplitude on the sphere is given by

$$\psi_k(X, Y, Z) = \frac{1}{4\pi}\int_{-\infty}^{+\infty} dz_o \int_{-\infty}^{+\infty} dx_o \left[\frac{\exp - ikr}{r}\left(-\frac{\partial\psi}{\partial y_o}\right) + \psi(x_o, y_o, z_o)\frac{\partial}{\partial y_o}\frac{\exp - ikr}{r}\right]_{y_o=0} \tag{21}$$

$$r = [(X - x_o)^2 + (Y - y_o)^2 + (Z - z_o)^2]^{\frac{1}{2}}$$

corresponding to the usual Green's function solution for an outgoing wave from a source in the x_o, z_o plane. Making the far-field approximations x_o/R, $z_o/R \lll 1$ and $kR \ggg 1$, where applicable, and performing the integration yields for the far-field amplitude

$$\psi_k = \psi_o \frac{ik \exp - ikR}{8R}[\cos\theta_o + \cos\theta\cos\varphi]\left(\frac{w_o^2}{\ln 2 \cos\theta_o}\right) \times \exp - \frac{k^2 w_o^2}{8 \ln 2}[(\cos\theta \sin\varphi)^2 + (\sin\theta_o - \sin\theta)^2/\cos^2\theta_o] \tag{22}$$

which can be recognized as the angular dependence of a Gaussian beam including the obliquity factor. The time-dependence is exp $i2\pi\nu t$.

The diffracted beam of frequency $\nu + f$ arises from a perturbation in the optical polarizability of the medium interacting with an optical beam moving at angle $-\theta_o$. The perturbation is proportional to the strain amplitude of the acoustic beam through the appropriate components of the photoelastic tensor. The volume polarization, at frequency $\nu + f$, in the limit of scattering sufficiently weak that the local field amplitude of the incident beam is essentially unchanged by the presence of the acoustic wave, may be written

$$\rho(x_o, y_o, z_o) \exp i2\pi(\nu + f)t = \psi_k(x_o, y_o, z_o, -\theta_o) \exp (i2\pi\nu t) S_o \exp i(2\pi f t - Kx_o) \quad -\tfrac{1}{2}L \leqq y_o \leqq \tfrac{1}{2}L \qquad -\tfrac{1}{2}h \leqq z_o \leqq \tfrac{1}{2}h \tag{23}$$

and zero otherwise. A rectangular acoustic beam of width L and height h, moving along the x_o-axis, has been assumed. The constant S_o represents the perturbed susceptibility which is proportional to the strain amplitude. The function $\psi_k(x_o, y_o, z_o, -\theta_o)$ is given by (20) with the appropriate change in the sign of θ_o. The diffracted beam amplitude at frequency $\nu + f$ and propagation constant $k' = 2\pi(\nu + f)/c'$ may be written

$$\psi_{k'}(X, Y, Z) = \int_{-\infty}^{+\infty} dx_o \int_{-\frac{1}{2}L}^{+\frac{1}{2}L} dy_o \int_{-\frac{1}{2}h}^{+\frac{1}{2}h} dz_o \rho(x_o, y_o, z_o) \frac{\exp - ik'r}{r} \tag{24}$$

corresponding to the volume Green's function solution for an outgoing wave.

The integral in (24) may be evaluated in a straightforward but lengthy fashion to yield

$$\psi_{k'} = \psi_o S_o \frac{\exp - ik'R}{R} \left(\frac{\pi L}{\beta}\right) \text{ReErf}\left[\tfrac{1}{2}\beta^{\frac{1}{2}}\left(h - \frac{ik' \cos\theta \sin\varphi}{\beta}\right)\right]$$

$$\times \frac{\sin(\xi - \eta \tan\theta_o)L/2}{(\xi - \eta \tan\theta_o)L/2} \exp - \frac{k'^2}{4\beta}\left[\cos^2\theta \sin^2\varphi + \frac{\eta^2}{k'^2 \cos^2\theta_o}\right], \quad (25)$$

in which

$$\beta = \frac{2 \ln 2}{w_o^2},$$

$$\eta = k' \sin\theta + k \sin\theta_o - K,$$

$$\xi = k' \cos\theta \cos\varphi - k \cos\theta_o,$$

and ReErf(z) is the real part of the error function of complex argument. It may be shown that for the parameters of interest one can make the approximation

$$\text{ReErf}\left[\tfrac{1}{2}\beta^{\frac{1}{2}}\left(h - \frac{ik' \cos\theta \sin\varphi}{\beta}\right)\right] \approx \text{Erf}\,[\tfrac{1}{2}\beta^{\frac{1}{2}}h]$$

with negligible error.

Except for constant factors the photocurrent may be written

$$\imath(f) = R^2 \int_0^{2\pi} d\varphi \int_{-\pi/2}^{\pi/2} d\theta \cos\theta \psi_{k'} \psi_k^* \quad . \quad (26)$$

The integral in (26) may be evaluated using (25) and (22). After appropriate manipulations the expression for the photocurrent takes the form

$$\imath(f) = -\frac{i}{8 \ln 2}\left(\frac{\pi^3}{\sin\theta_o}\right)^{\frac{1}{2}} P_{\text{optical}}(P_{\text{acoustic}})^{\frac{1}{2}} \exp i2\pi f(t - R/c')$$

$$\times \left[\frac{\text{Erf}\,[(\tfrac{1}{2}\ln 2)^{\frac{1}{2}}h/w_o]}{[(\tfrac{1}{2}\ln 2)^{\frac{1}{2}}h/w_o]^{\frac{1}{2}}}\right]\left[\frac{\text{Erf}\,[(\ln 2)^{\frac{1}{2}}(L/w_o)\sin\theta_o]}{[(\ln 2)^{\frac{1}{2}}(L/w_o)\sin\theta_o]^{\frac{1}{2}}}\right] \quad (27)$$

$$\times \exp - \frac{\pi^2(f - f_o)^2 w_o^2}{4 \ln 2 v^2 \cos^2\theta_o},$$

in which

$$f_o = (2v/\lambda) \sin\theta_o$$

is the optimum frequency for Bragg diffraction and

$$P_{\text{optical}} = \pi w_o^2 \mid \psi_o \mid^2$$

$$P_{\text{acoustic}} = Lh \mid S_o \mid^2.$$

REFERENCES

1. Forrester, A. T., Gudmundsen, R. A., and Johnson, P. O., Photoelectric Mixing of Incoherent Light, Phys. Rev., *99,* 1955, p. 1691. See also, Forrester, A. T., Mixing as a Spectroscopic Tool, J. Opt. Soc. Amer., *51,* 1961, p. 253.
2. Javan, A., Bennet, Jr., W. R., and Herriott, D. R., Population Inversion and Continuous Optical Maser Oscillation in a Gas Discharge Containing a He-Ne Mixture, Phys. Rev. Letters, *6,* 1961, p. 106. See also, Javan, A., Billik, E. A., and Bond, W. L., Frequency Characteristics of a Continuous-Wave He-Ne Optical Maser, J. Opt. Soc. Amer., *52,* 1962, p. 96.
3. Jennings, D. A. and Takuma, H., Optical Heterodyne Delection of the Forward-Stimulated Brillouin Scattering, Appl. Phys. Letters, *5,* 1964, p. 241; Lastovka, J. B. and Benedek, G. B., *Physics of Quantum Electronics Conference Proceedings,* ed. Kelley, Lax and Tannenwald, McGraw-Hill Book Company, Inc., New York, 1966, p. 231.
4. Cummins, H. Z., Knable, N., and Yeh, Y., Observation of Diffusion Broadening of Rayleigh Scattered Light, Phys. Rev. Letters, *12,* 1964, p. 150.
5. Cummins, H. Z. and Knable, N., Single Sideband Modulation of Coherent Light by Bragg Reflection from Acoustic Waves, Proc. IEEE, *51,* 1963, p. 1246.
6. Goodwin, F. E. and Pedinoff, M. E., Application of CCl_4 and CCl_2:CCl_2 Ultrasonic Modulators to Infrared Optical Heterodyne Experiments, Appl. Phys. Letters, *8,* 1966, p. 60.
7. Cohen, M. G. and Gordon, E. I., Acoustic Beam Probing Using Optical Techniques, B.S.T.J., *44,* May–June, 1965, p. 693.
8. Lucovsky, G., Lasser, M. E., and Emmons, R. B., Coherent Light Deflection in Solid-State Photodiodes, Proc. IEEE, *51,* 1963, p. 166.
9. Kösters, W., Interferenzdoppelprisma Für Messzwecke, Reichspatentamt Patentschrift Nr. 595211, 1931.
10. Saunders, J. B., The Kösters Interferometer, J. Research Nat. Bur. Stand., *58,* 1957, p. 27.
11. Kogelnik, H., Imaging of Optical Modes-Resonators with Internal Lenses, B.S.T.J., *44,* March, 1965, p. 455.
12. Foster, N. F., Cadmium Sulfide Evaporated-Layer Transducers, Proc. IEEE, *53,* 1965, p. 1400.
13. Gordon, E. I. and Cohen, M. G., Electro-Optic Diffraction Grating for Light Beam Modulation and Diffraction, IEEE J. Quantum Electron., *QE-1,* 1965, p. 191. The quantity $\eta^{\frac{1}{2}} \equiv \xi L$, where ξ is defined in this reference as the incremental phase shift per unit length produced by the acoustic wave.